Inorg. Chem. **2004**, *43*, 5403–5409

Synthesis, Structure, and Substitution Mechanism of New Ru(II) Complexes Containing 1,4,7-Trithiacyclononane and 1,10-Phenanthroline Ligands

Xavier Sala, Isabel Romero, Montserrat Rodríguez, and Antoni Llobet*

Departament de Química, Universitat de Girona, Campus de Montilivi, E-17071 Girona, Spain

Gabriel González*

Departament de Química Inorgànica, Universitat de Barcelona, Martí i Franquès 1-11, E-08028 Barcelona, Spain, and Institut Catal d'Investigaci Quimica (ICIQ, Avgda. Pasos Catalans s/n, E-43007 Tarragon, Spain

Manuel Martínez

Department de Quimica Inorgànica, Universitat de Barcelona, Martí Franquès 1-11, E-08028 Barcelona, Spain

Jordi Benet-Buchholz

BIS-SUA-SPA X-ray Laboratory, Geb. Q18; Bayer Industry Services, D-51368 Leverkusen, Germany, and Institut Catal d'Investigaci Quimica (ICIQ, Avgda. Pasos Catalans s/n, E-43007 Tarragon, Spain

Received February 25, 2004

Two new Ru complexes containing the 1,10-phenanthroline (phen) and 1,4,7-trithiacyclononane ([9]aneS$_3$, $\overline{SCH_2CH_2SCH_2CH_2SCH_2CH_2}$) ligands of general formula [Ru(phen)(L)([9]aneS$_3$)]$^{2+}$ (L = MeCN, **3**; L = pyridine (py), **4**) have been prepared and thoroughly characterized. Structural characterization in the solid state has been performed by means of X-ray diffraction analyses, which show a distorted octahedral environment for a diamagnetic d^6 Ru(II), as expected. ^{1}H NMR spectroscopy provides evidence that the same structural arrangement is maintained in solution. Further spectroscopic characterization has been carried out by UV–vis spectroscopy where the higher π acceptor capability of MeCN versus the py ligand is manifested in a 9–15-nm blue shift in its MLCT bands. The $E_{1/2}$ redox potential of the Ru(III)/Ru(II) couple for **3** is anodically shifted with respect to its Ru–py analogue, **4**, by 60 mV, which is also in agreement with a higher electron-withdrawing capacity of the former. The mechanism for the reaction Ru–py + MeCN → Ru–MeCN + py has also been investigated at different temperatures with and without irradiation. In the absence of irradiation at 326 K, the thermal process gives kinetic constants of $k_2 = 1.4 \times 10^{-5}$ s^{-1} ($\Delta H^{\ddagger} = 108 \pm 3$ kJ mol^{-1}, $\Delta S^{\ddagger} = -8 \pm 9$ J K^{-1} mol^{-1}) and $k_{-2} = 2.9 \times 10^{-6}$ s^{-1} ($\Delta H^{\ddagger} = 121 \pm 1$ kJ mol^{-1}, $\Delta S^{\ddagger} = 18 \pm 3$ J K^{-1} mol^{-1}). The phototriggered process is faster and consists of preequilibrium formation of an intermediate that thermally decays to the final Ru–MeCN complex with an apparent rate constant of $(k_1 K_{h\nu})_{app} = 1.8 \times 10^{-4}$ s^{-1} at 304 K, under the continuous irradiation experimental conditions used.

Introduction

Ru(II) polypyridylic complexes represent a keystone in the development of photochemistry and electron- and energy-transfer disciplines,[1] which among other applications have led to the design of molecular electronics,[2] including wires and switches.[3] Furthermore, Ru(II) polypyridyl complexes are often used as building blocks for the development of macromolecular assemblies that are of interest in biochemistry and clinical diagnosis[4] as well as for the design of molecular machines.[5] In most of the above-mentioned areas,

* Authors to whom correspondence should be addressed. E-mail: antoni.llobet@udg.es (A.L.); gabriel.gonzalez@qu.ub.es (G.G.).

10.1021/ic0497533 CCC: $27.50
Published on Web 07/24/2004

the synthetic strategy followed to obtain the desired compounds is via Ru(II) substitution chemistry.[6] Unfortunately, full mechanistic studies of these reactions are scarce and, in many cases, incomplete.[7] As a result of these two factors, it is of primary importance to understand and control the electronic and steric factors exerted by different types of ligands to monitor their substitution processes properly.

Recently, new Ru(II) heteroleptic pyridyl and nitrile complexes containing the macrocyclic sulfur-donor ligand 1,4,7-trithiacyclononane ([9]aneS$_3$, $\overline{SCH_2CH_2SCH_2CH_2SCH_2CH_2}$), with general formula $[Ru(py)_x(MeCN)_{3-x}([9]aneS_3)]^{2+}$ ($x = 1-3$), have been described in the literature.[8] Their substitution chemistry has been qualitatively described, and surprisingly, the nitrile complexes are easily formed from pyridylic synthetic intermediates. This turns out to be the opposite of the general method that is commonly employed.[8] In view of these results and with the aim of gaining further insight into the substitution mechanisms of $[Ru^{II}N_3S_3]$-type complexes, we present in this paper the preparation and structural characterization of two new Ru(II) compounds of formula $[Ru(phen)(L)([9]aneS_3)]^{2+}$ (phen = 1,10-phenanthroline and L = py, MeCN). Their spectroscopic and electrochemical properties are also described, and a full mechanistic study of their substitution chemistry has been performed. This study has allowed us to not only establish a definite reaction scheme for a not-so-simple substitution process but also tentatively identify the intermediate species that is generated upon photochemical irradiation.[9]

Experimental Section

Materials. All reagents were obtained from Aldrich Chemical Co. and were used without further purification. Reagent-grade organic solvents were obtained from SDS, and high-purity deionized water was obtained from a nanopure Milli-Q water purification system.

Compounds. $[Ru(Cl)(phen)([9]aneS_3)]Cl$ (**1**) and $[Ru(phen)(OH_2)([9]aneS_3)](ClO_4)_2$ (**2**) complexes were prepared according to literature procedures.[10] All synthetic manipulations were carried out under a nitrogen atmosphere using Schlenck and vacuum line techniques.

$[Ru(phen)(MeCN)([9]aneS_3)](ClO_4)_2 \cdot 0.5EtOH$ **(3·0.5EtOH).** This complex was prepared following two alternative synthetic routes.

(A) A 50.0-mg (0.074 mmol) sample of $[Ru(phen)(OH_2)([9]aneS_3)](ClO_4)_2$ was dissolved in 20 cm^3 of CH_3CN and maintained under vigorous stirring for 10 min at room temperature. After the addition of 5 cm^3 of Et_2O, a pale-yellow precipitate formed. This precipitate was filtered, washed with a small amount of cold acetonitrile, and dried under vacuum. The solid obtained in this way was then recrystallized from room-temperature ethanol. Yield, 43.1 mg (80.7%). Anal. Calcd for $C_{20}H_{23}Cl_2O_8N_3RuS_3 \cdot 0.5C_2H_6O$: C, 34.90 (34.81); H, 3.30 (3.62); N, 5.88 (5.79); S, 13.05 (13.25). ^{1}H NMR (CD_3CN, 200 MHz): δ 9.33 (dd, $J_{2-3} = 5.2$ Hz, $J_{2-4} = 1.2$ Hz, H2, H11), 8.80 (dd, $J_{4-3} = 8.4$ Hz; $J_{4-2} = 1.2$ Hz, H4, H9), 8.27 (s, H6, H7), 8.08 (dd, $J_{3-2} = 5.2$ Hz, $J_{3-4} = 8.4$ Hz, H3, H10), 3.5−2.5 (m, 12H [9]aneS3). $E_{1/2}(CH_3CN) = 1.68$ V versus SSCE. UV−vis (MeCN): λ_{max}, nm (ϵ, M^{-1} cm^{-1}) 223 (33205) sh, 256 (32322), 285 (14499) sh, 345 (5135), 396 (4047).

(B) A 50.0-mg (0.067 mmol) sample of $[Ru(phen)(py)([9]aneS_3)](ClO_4)_2$ (**4**) was dissolved in 20 cm^3 of CH_3CN under vigorous stirring and the solution was irradiated with a 100-W tungsten lamp. After 4 h, 5 cm^3 of Et_2O was added, and a pale-yellow precipitate appeared. This precipitate was filtered, washed with a small amount of cold acetonitrile, and dried under vacuum. Yield, 43.3 mg (88.6%). Anal. Calcd for $C_{20}H_{23}Cl_2O_8N_3RuS_3 \cdot 0.5C_2H_6O$: C, 34.90 (34.81); H, 3.30 (3.62); N, 5.88 (5.79); S, 13.05 (13.25).

$[Ru(phen)(py)([9]aneS_3)](ClO_4)_2$ **(4).** To a solution of 80.0 mg (0.118 mmol) of **2** in 100 cm^3 of water, we added 0.284 cm^3 of pyridine. The resulting mixture was stirred at room temperature for 3 days, and then 2 cm^3 of a saturated aqueous solution of NH_4-

(1) (a) Ramamurthy, V., Schanze, K. S., Eds. *Organic and Inorganic Photochemistry*; Marcel Dekker: New York, 1998. (b) Thompson, D. W.; Schoonover, J. R.; Graff, D. K.; Fleming, C. N.; Meyer, T. J. *J. Photochem. Photobiol., A* **2000**, *137*, 131−134. (c) Toma, H. E.; Serrasqueiro, R. M.; Rocha, R. C.; Demets, G. J. F.; Winnischofer, H.; Araki, K.; Ribeiro, P. E. A.; Donnici, C. L. *J. Photochem. Photobiol., A* **2000**, *135*, 185−191. (d) Keefe, M. H.; Benkstein, K. D.; Hupp, J. T. *Coord. Chem. Rev.* **2000**, *205*, 201−228. (e) Romero, M. I.; Rodríguez, M.; Llobet, A.; Collomb-Dunand-Sauthier, M. N.; Deronzier, A.; Parella, T.; Stoeckli-Evans, H. *J. Chem. Soc., Dalton Trans.* **2000**, 1689−1694. (f) Tyson, D. S.; Luman, C. R.; Zhou, X.; Castellano, F. N. *Inorg. Chem.* **2001**, *40*, 4063−4071. (g) Balzani, V.; Juris, A. *Coord. Chem. Rev.* **2001**, *211*, 97−115. (h) Dattelbaum, D. M.; Hartshorn, C. M.; Meyer, T. J. *J. Am. Chem. Soc.* **2002**, *124*, 4938−4939. (i) Nikolau, S.; Toma. H. E. *J. Chem.* Soc., *Dalton Trans.* **2002**, 352−359.

(2) (a) Hatzidimitriou, A.; Gourdon, A.; Devillers, J.; Launay, J. P.; Mena, E.; Amouyal, E. *Inorg. Chem.* **1996**, *35*, 2212−2219. (b) Balzani, V.; Credi, A.; Venturi, M. *Chem.—Eur. J.* **2002**, *8*, 5524−5532.(c) Camera, S. G.; Toma, H. E. *J. Photochem. Photobiol., A* **2002**, *151*, 57−65.

(3) (a) Balzani, V.; Scandola, F. *Supramolecular Photochemistry*; Ellis Horwood: Chichester, U.K., 1991. (b) Sauvage, J. P.; Collin, J. P.; Chambron, J. C.; Guillerez, S.; Coudret, C. *Chem. Rev.* **1994**, *94*, 993−1019. (c) Brennaman, M. K.; Alstrumacevedo, J. H.; Fleming, C. N.; Jang, P.; Meyer, T. J.; Papanikolas, J. M. *J. Am. Chem. Soc.* **2002**, *124*, 15094−15098.

(4) (a) Friedman, A. E.; Chambron, J. C.; Sauvage, J. P.; Turro, N. J.; Barton, J. K. *J. Am. Chem. Soc.* **1990**, *112*, 4960−4962. (b) Jenkis, Y.; Friedman, A. E.; Turro, N. J.; Barton, J. K. *Biochemistry* **1992**, *21*, 809−816. (c) Holmlin, R. E.; Stemp, E. D. A.; Barton J. K. *Inorg. Chem.* **1998**, *37*, 29−34. (d) Li, L.; Szmacinski, H.; Lakowicz, J. R. *Biospectroscopy* **1997**, *3*, 155−159. (e) Li, L.; Szmacinski, H.; Lakowicz, J. R. *Anal. Biochem.* **1997**, *244*, 80−85. (f) Terpetschnig, E. Szmacinski, H.; Lakowicz, J. R. *Anal. Biochem.* **1995**, *227*, 140−147. (g) Youn, H.; Terpetschnig, E.; Szmacinski, H.; Lakowicz, J. R. *Anal. Biochem.* **1995**, *232*, 24−30. (h) Murtaza, Z.; Chang, Q.; Rao, G.; Lin, H.; Lakowicz, J. R. *Anal. Biochem.* **1997**, *247*, 216−222. (i) Santos, T. M.; Goodfellow, B. J.; Drew, M. G. B.; Pedrosa de Jesus, J.; Félix, V. *Metal Based Drugs* **2001**, *8*, 125−136.

(5) (a) Sauvage, J. P. *Acc. Chem. Res.* **1998**, *31*, 611−619. (b) Balzani, V.; Gomez-López, M.; Stoddart, J. F. *Acc. Chem. Res.* **1998**, *31*, 405−414. (c) *Struct. Bonding (Berlin)* 2001, *99*, 1−281 (special volume on "Molecular Machines and Motors"). (d) Balzani, V.; Credi, A.; Raymo, F. M.; Stoddart, J. F. *Angew. Chem., Int. Ed.* **2000**, *39*, 3349−3391. (e) Collin, J. P.; Dietrich-Buchecker, C.; Gaviña, P.; Jiménez-Molero, M. C.; Sauvage, J. P. *Acc. Chem. Res.* **2001**, *34*, 477−487.

(6) (a) Sullivan, B. P.; Calvert, J. M.; Meyer, T. J. *Inorg. Chem.* **1980**, *19*, 1404−1407. (b) Silva, M.; Tfouni, E. *Inorg. Chem.* **1997**, *36*, 274−277. (c) Malouf, G.; Ford, P. C. *J. Am. Chem. Soc.* **1977**, *26*, 7213−7221. (d) Laemmel, A. C.; Collin, J. P.; Sauvage, J. P. *R. Acad. Sci. Paris* **2000**, *3*, 43−49. (e) Matsubara, T.; Creutz, C. J. *Am. Chem. Soc.* **1979**, *18*, 1956−1966.

(7) (a) Arakawa, R.; Abe, K.; Abura, T.; Nakabayashi, Y. *Bull. Chem. Soc. Jpn.* **2002**, *75*, 1983−1989. (b) Bessel, C. A.; Margarucci, J. A.; Acquaye, J. H.; Rubino, R. S.; Crandall, J.; Jircitano, A. J.; Takeuchi, K. J. *Inorg. Chem.* **1993**, *32*, 5779−5784.

(8) Roche, S.; Adams, H.; Spey, S. E.; Thomas, J. A. *Inorg. Chem.* **2000**, *39*, 2385−2390.

(9) (a) Baranoff, E.; Collin, J. P.; Furusho, J.; Furusho, Y.; Laemmel, A. C.; Sauvage, J. P. *Inorg. Chem.* **2002**, *41*, 1215−1222.(b) Schofield, E. R.; Collin, J. P.; Gruber, N.; Sauvage, J. P. *Chem. Commun.* **2003**, 188−189.

(10) (a) Goodfellow, B. J.; Félix, V.; Pacheco, S. M.; Pedrosa de Jesus, J.; Drew, M. G. B. *Polyhedron* **1997**, *16*, 393−401. (b) Sala, X.; Poater, A.; Romero, I.; Rodríguez, M.; Llobet, A.; Solans, X.; Parella, T.; Santos, M. T. *Eur. J. Inorg. Chem.* **2004**, 612−618.

ClO_4 was added. The resulting solution was left standing overnight, upon which a yellow solid was formed. This solid was filtered, washed with cold water, and dried under vacuum. Yield: 63.0 mg (72.2%). Anal. Calcd for $C_{23}H_{25}Cl_2O_8N_3RuS_3$: C, 37.21 (37.36); H, 3.40 (3.38); N, 5.52 (5.68); S, 12.87(13.01). ^{1}H NMR (CD_3CN, 200 MHz): δ 9.57 (dd, $J_{2-3} = 5.2$ Hz; $J_{2-4} = 1$ Hz, H2, H11), 8.80 (dd, $J_{4-3} = 8.2$ Hz, $J_{4-2} = 1.2$ Hz, H4, H9), 8.66 (d, $J_{23-24} = 5.2$ Hz, H23, H27), 8.21 (s, H6, H7), 8.14 (dd, $J_{3-2} = 5.2$ Hz, $J_{3-4} = 8.2$ Hz, H3, H10), 7.75 (t, H25), 7.27 (t, H24, H26), 3.64−2.5 (m, 12H [9]aneS3). $E_{1/2}$(MeCN) = 1.62 V versus SSCE. UV−vis (MeCN): λ_{max}, nm (ϵ, M^{-1} cm^{-1}) 220 (32263) sh, 259 (35616), 286 (19793) sh, 354 (4641), 411 (4394).

Instruments. UV−vis spectroscopy was carried out in a diode array HP-89532A or in a Cary50 spectrophotometer. pH measurements were monitored using a Micro-pH-2000 from Crison. Cyclic voltammetric experiments were carried out in a PAR 263A EG&G potentiostat using a three-electrode cell; glassy carbon-disk electrodes (3-mm diameter) from BAS were used as the working electrode, platinum wire was used as the auxiliary electrode, and SSCE was used as the reference electrode. All cyclic voltammograms were recorded at a scan rate of 100 mV/s under a nitrogen atmosphere after dissolving the complexes (approximately 1×10^{-3} M) in degassed solvents containing the necessary amount of (n-Bu_4N)(PF_6) as the supporting electrolyte to produce a 0.1 M ionic strength solution. Reported $E_{1/2}$ values are ($E_{p,a} + E_{p,c}$)/2.

^{1}H NMR spectroscopy was carried out on a Bruker DPX 200 MHz instrument in acetonitrile-d_3 using internal references. Elemental analyses were performed using a CHNS−O elemental analyzer EA-1108 from Fisons.

X-ray Structure Determination. Suitable yellow crystals (prisms or needles) of [Ru(phen)(MeCN)([9]aneS3)](ClO_4)$_2$ (**3**) or [Ru(phen)(py)([9]aneS3)](ClO_4)$_2$·H_2O (**4**·H_2O) were obtained upon the slow diffusion of ether into a saturated dichloromethane solution containing these complexes for 2 days.

Data Collection. Measurements were made on a Siemens P4 diffractometer equipped with a SMART-CCD-1000 area detector, a MACScience Co. rotating anode with Mo Kα radiation, a graphite monochromator, and a Siemens LT2 low-temperature device (T = −120 °C). The measurements were made in the range of 1.55−30.00° for **3** and 1.90−31.51° for **4**. For **3**, a total of 148242 reflections were collected of which 29676 are unique (R_{int} = 0.1249), and for **4**, a total of 21001 reflections were collected, of which 8381 are unique (R_{int} = 0.0553). Full-sphere data collection was used with ω and φ scans. Programs used are as follows: data collection, Smart V. 5.060 (BrukerAXS 1999); data reduction, Saint + version 6.02 (Bruker AXS 1999); absorption correction, SADABS (Bruker AXS 1999).

Structure Solution and Refinement. The package SHELXTL version 5.10 was used.[11]

Kinetic Measurements. All kinetic measurements were monitored by UV−vis spectroscopy in the full 500−300-nm range on an HP8452A diode-array instrument equipped with a multicell transport thermostated (±0.1 °C) with a circulating bath; some experiments were also run with a TIDAS instrument on thermostated cells. Despite the fact that the intensity of the lamp used in the latter instrument was much higher, we found that the values obtained for the observed rate constants were the same as those for the experiments run on the HP8452A instrument. The rate constants were derived from exponential least-squares fitting by the standard routines. When constant irradiation of the sample was required, we performed the kinetic runs with the instrument shutter open; alternatively, when no irradiation of the sample was required, we performed the kinetic runs with the instrument shutter closed between measurements, and the instrument was kept in the dark during the entire kinetic run. All runs were performed under pseudo-first-order conditions; solutions for the kinetic runs were prepared by mixing the calculated amounts of thermostated solutions of the ruthenium compound and acetonitrile or/and pyridine. The observed rate constants were derived from the absorbance versus time traces at the wavelengths where a maximum increase and/or decrease of absorbance was observed. No differences in the values obtained for k_{obs} were detected for different wavelengths, as expected for reactions where a good retention of isosbestic points is observed; furthermore, no differences in these values were detected when using single- or global-wavelength analysis.[12] The general kinetic technique used in the present work has been previously described elsewhere.[13] The obtained k_{obs} values are given as Supporting Information (Table S1).

Table 1. Crystal Data for Complexes **3** and **4** and Related Complexes

	3	**4**
empirical formula	$C_{80}H_{92}Cl_8N_{12}O_{32}Ru_4S_{12}$	$C_{23}H_{27}Cl_2N_3O_9RuS_3$
formula weight	2806.26	757.63
cryst syst, space group	monoclinic, $P2_1/c$	triclinic, $P\bar{1}$
A, Å	14.3977(10)	11.0103(4)
B, Å	33.495(3)	11.7826(4)
C, Å	21.2512(16)	12.0065(4)
α, deg	90	64.4410(10)
β, deg	95.880(3)	76.3940(10)
γ, deg	90	83.7040(10)
V, Å^3	10194.4(13)	1365.68(8)
formula units/cell	4	2
ρ_{calcd}, g cm^{-3}	1.828	1.842
μ, mm^{-1}	1.123	1.058
R1[a] ($I > 2\sigma(I)$)	0.0762	0.0436
	0.1847	0.1189
wR2[b] (all data)	(m = 0.1023;	(m = 0.0747;
	n = 15.2289)	n = 1.4389)

[a] $R1 = \Sigma||F_o| - |F_c||/\Sigma|F_o|$. [b] $wR2 = [\Sigma\{w(F_o^2-F_c^2)^2\}/\Sigma\{w(F_o^2)^2\}]^{1/2}$, where $w = 1/[\sigma^2F_o^2+(m)^2+n\mathrm{P}]$ and $\mathrm{P} = (F_o^2 + 2F_c^2)/3$.

Results and Discussion

Synthesis and Solid-State Structure. The addition of a Ag(I) salt to the Ru−Cl complex, **1**, generates the Ru−H_2O complex, **2**, in nearly quantitative yield. This complex, if dissolved in acetonitrile, forms the Ru-MeCN complex, **3**. Complex **4** can be obtained by dissolving any of the complexes described above in pyridine.

Crystallographic data and selected bond distances and angles for complexes **3** and **4** are presented in Tables 1 and 2, respectively; ORTEP views together with their labeling schemes are depicted in Figure 1. Because of the presence of the [9]aneS$_3$ ligand, the Ru−MeCN complex, **3**, presents two pairs of $\lambda\lambda\lambda$ and $\delta\delta\delta$ conformomers within the unit cell with slightly different metric parameters. Thus, only the so-called "A" ($\delta\delta\delta$) complex will be described here.

It is worth mentioning that in the cationic moiety of complex **3** the [9]aneS$_3$ ligand coordinates facially through the sulfur atoms in an endodentate manner. The bond

(11) *SHELXTL*, version 5.10; Universität Göttingen: Göttingen, Germany, 1998.

(12) Binstead, R. A.; Zuberbühler, A. D. *Specfit*, version 3.0.32; Spectrum Software Associates: Marlborough, U.K., 1996.

(13) Benzo, F.; Bernhardt, P. V.; González, G.; Martinez, M.; Sienra, B. *J. Chem. Soc., Dalton Trans.* **1999**, 3973−3979.

Table 2. Selected Bond Lengths (Å) and Angles (deg) for Complexes **3** and **4**

complex **3**[a]		complex **4**	
Ru1−N1	2.051(6)	Ru1−N1	2.098(2)
Ru1−N12	2.098(5)	Ru1−N12	2.0936(19)
Ru1−N21	2.106(5)	Ru1−N22	2.1163(19)
Ru1−S2	2.2755(19)	Ru1−S2	2.3019(5)
Ru1−S1	2.2947(16)	Ru1−S1	2.3005(5)
Ru1−S3	2.3037(17)	Ru1−S3	2.3043(6)
N1−Ru1−N12	78.7(2)	N1−Ru1−N12	78.92(8)
N1−Ru1−N21	89.3(2)	N1−Ru1−N22	92.03(8)
N12−Ru1−N21	89.2(2)	N12−Ru1−N22	89.67(7)
N1−Ru1−S2	91.69(16)	N1−Ru1−S2	90.58(5)
N12−Ru1−S2	93.70(16)	N12−Ru1−S2	92.75(5)
N21−Ru1−S2	177.10(16)	N22−Ru1−S2	176.73(6)
N1−Ru1−S1	99.53(15)	N1−Ru1−S1	96.67(5)
N12−Ru1−S1	177.48(16)	N12−Ru1−S1	175.55(6)
N21−Ru1−S1	89.05(16)	N22−Ru1−S1	89.88(6)
S2−Ru1−S1	88.08(8)	S2−Ru1−S1	87.87(2)
N1−Ru1−S3	172.98(15)	N1−Ru1−S3	175.28(5)
N12−Ru1−S3	94.35(15)	N12−Ru1−S3	96.61(6)
N21−Ru1−S3	90.09(16)	N22−Ru1−S3	89.42(6)
S2−Ru1−S3	89.36(7)	S2−Ru1−S3	88.12(2)
S1−Ru1−S3	87.44(16)	S1−Ru1−S3	89.82(2)

[a] Selected molecule with code A.

distances and angles are within the expected values for this type of complex.[10,14] All cis angles involving Ru as the central atom are very close to the expected 90° for an ideal octahedral geometry with the logical exception of the N1Ru1N12 angle of the phen ligand, which is shorter. The structural features of complex **4** are relatively similar to those of **3**, and thus, they will not be described in detail.

The cationic moieties are electrostatically balanced by perchlorate counteranions; in **3**, all of them are highly disordered, whereas in **4**, only one is disordered.

At this point, it is of particular interest to compare the bonding metric parameters of related complexes, namely, $[Ru(py)_2(MeCN)([9]aneS_3)]^{2+}$ (**5**), $[Ru(py)_3([9]aneS_3)]^{2+}$ (**6**) and $[Ru(py)_3(tpm)]^{2+}$ (**7**), (tpm is the tridentate facial ligand tris(1-pyrazolyl)methane)[8,15] because it has implications with regard to their chemical behavior. In comparing complexes **6** and **7**, it is found that the mean value for the Ru−N(py) bond is 4.6(6) pm longer for the former than for the latter; a similar trend is also observed in the Ru−py distance of **4** that is 3.2(6) pm longer than that of the mean value for **7**. This effect has to be related to the electronic characteristics of the [9]aneS$_3$ ligand[10b,16] and probably also applies to the Ru−NCMe bond.

Spectral and Redox Properties. The ^{1}H NMR spectra of complexes **3** and **4** were registered in MeCN-d_3 and are assigned in the Experimental Section; their aromatic region is presented in Figure 2. All of the resonances in the NMR spectra were unambiguously identified and are consistent with the same structure found in the solid state for both complexes.

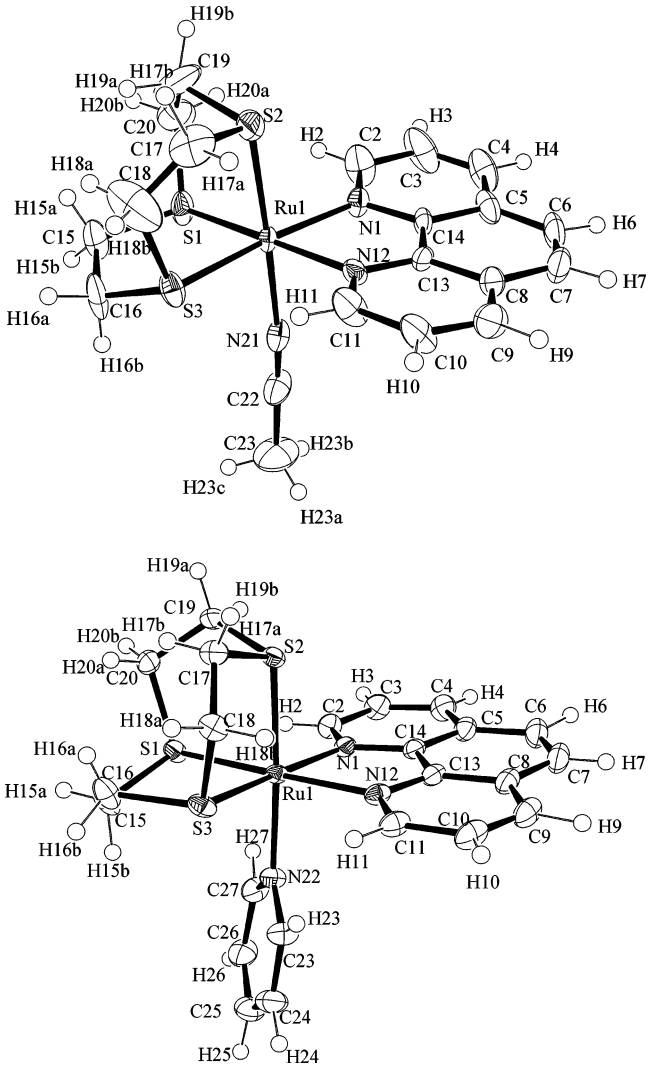

Figure 1. ORTEP view (ellipsoids are drawn at the 50% probability level) of the molecular structure of cations **3** and **4**, including the atom numbering scheme.

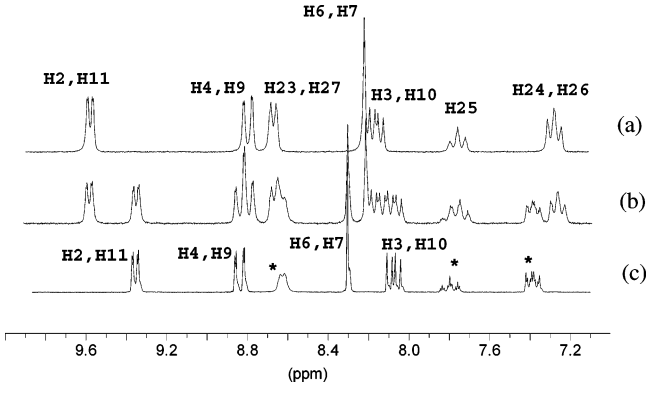

Figure 2. ^{1}H MNR monitoring (aromatic region) of the irradiation process of complex **4** (a) before irradiation, (b) after the disappearance of approximately half of complex **4**, and (c) after the complete disappearance of complex **4** with the formation of complex **3′** and free pyridine (resonances of the latter are indicated with asterisks).

(14) (a) Santos, T. M.; Goodfellow, B. J.; Madureira, J.; Pedrosa de Jesus, J.; Félix, V.; Drew, M. G. B. *New J. Chem.* **1999**, *23*, 1015−1025. (b) Madureira, J.; Santos, T. M.; Goodfellow, B. J.; Lucena, M. J.; Pedrosa de Jesus, J.; Santana-Marques, M. G.; Drew, M. G. B.; Félix, V. *J. Chem. Soc., Dalton Trans.* **2000**, 4422−4431. (c) Llobet, A.; Curry, M.; Evans H. T.; Meyer, T. J. *Inorg. Chem.* **1989**, *28*, 3131−3137. (d) Llobet, A.; Hodgson, D. J.; Meyer, T. J. *Inorg. Chem.* **1990**, *29*, 3760−3766. (e) Sens, C.; Rodríguez, M.; Romero, I.; Llobet, A.; Parella, T.; Sullivan, B. P.; Benet-Buchholz, J. *Inorg. Chem.* **2003**, *42*, 2040−2048.

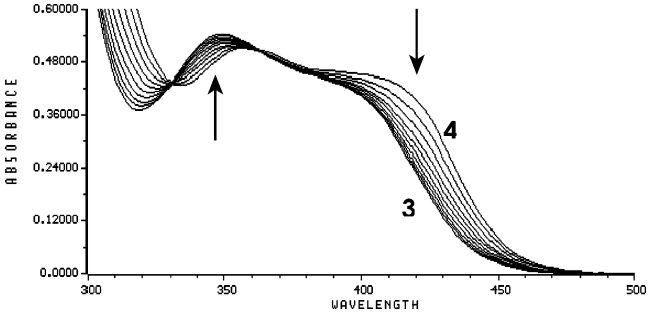

Figure 3. Evolution from complex **4** to **3** upon photochemical excitation of a solution of **4** in MeCN, [Ru] = 1.3×10^{-4} M.

The irradiation (white light) of **4** dissolved in deuteroacetonitrile produces the following solvolysis reaction

$$[\mathrm{Ru(phen)(py)([9]aneS_3)}]^{2+} + \mathrm{CD_3CN} \rightarrow \underset{\mathbf{4}}{} \qquad [\mathrm{Ru(phen)(CD_3CN)([9]aneS_3)}]^{2+} + \mathrm{py} \quad \underset{\mathbf{3'}}{}$$

In the absence of light, the reverse reaction only takes place very slowly. Figure 2 shows how this reaction can be qualitatively followed through NMR spectroscopy.

The electronic spectra of the Ru−MeCN (**3**) and Ru−py (**4**) complexes are shown in Figure 3. Below 300 nm, mainly ligand-based pyridine and/or phenanthroline $\pi-\pi^*$ transitions are observed. Above 300 nm, two bands appear at 345 nm (5135 M^{-1} cm^{-1}) and 396 nm (4047 M^{-1} cm^{-1}) for **3** and at 354 nm (4641 M^{-1} cm^{-1}) and 411 nm (4394 M^{-1} cm^{-1}) for **4** that can be assigned to a series of MLCT ($d\pi-\pi^*$(Ru−phen)) transitions and their vibronic components on the basis of the literature that is available for related complexes.[10a,17]

The redox properties were investigated by means of cyclic voltammetry producing quasireversible waves at $E_{1/2} = 1.68$ V ($E_{p,a} = 1.74$ V, $E_{p,c} = 1.62$ V, $\Delta E = 120$ mV) for Ru−MeCN complex **3** and at $E_{1/2} = 1.62$ V ($E_{p,a} = 1.66$ V, $E_{p,c} = 1.57$ V, $\Delta E = 90$ mV) for Ru−py complex **4**. This 60-mV shift is in accordance with the stronger π acceptor capability of the MeCN ligand with regard to pyridine.[8]

Mechanistic Study. When complex [Ru(phen)(py)([9]-aneS$_3$)](ClO$_4$)$_2$ (**4**) is dissolved in MeCN and irradiated with a constant intensity of white light, the substitution of the pyridine ligand by MeCN takes place producing [Ru(phen)-(MeCN)([9]aneS$_3$)]$^{2+}$ complex **3** according to NMR spectroscopy, as indicated above (Figure 2). The reaction progress can be monitored by UV−vis spectroscopy, which displays well-defined isosbestic points (Figure 3). Furthermore, the absorbance versus time traces at different wavelengths show a well-behaved first-order shape. However, a nonlinear Eyring plot is detected (Figure 4),[18] suggesting the presence of two different reactions in a temperature-dependence competition; in addition, the absorbance changes are also temperature dependent. Keeping in mind all of the above together with the preparative reaction pattern, the following equilibrium depicted in Scheme 1 can be suggested.

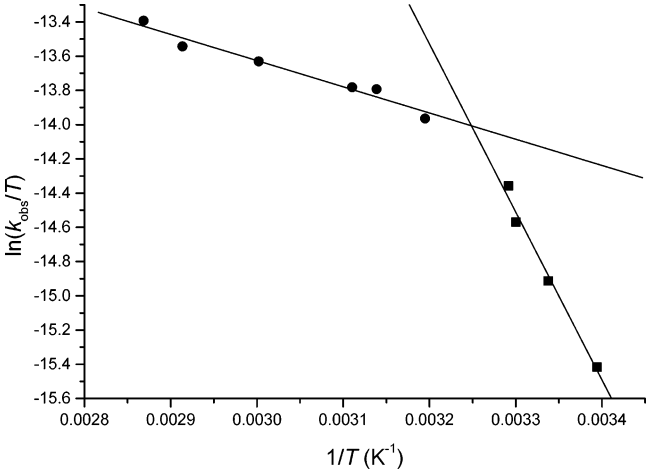

Figure 4. Plot of the temperature dependence of the observed rate constant for the process observed after photochemical excitation of [Ru(phen)(py)-([9]aneS$_3$)]$^{2+}$ in MeCN solution.

Upon continuous irradiation inside the spectrophotometer compartment, the Ru−py complex, **4**, is taken to a photochemical excited state, **4***, that immediately decays to an intermediate species in very low concentration. The available data suggest that this intermediate species has already suffered some bond rearrangement, similar to that of previously described examples reported in the literature.[19] The process can be described in steady-state pre-equilibrium terms where compound **4** exists in fast equilibrium with the above-mentioned intermediate via its photoexcited form, **4***. The fact that the intensity of the lamp used for continuous irradiation does not affect either the observed rate constants or the intensity of the spectral changes (see Experimental section) supports this hypothesis. After this photochemical process, the intermediate species evolves via path 1 to the Ru−NCMe complex, **3**, which reacts thermally to give back the initial complex, **4**, via two alternative routes (1 and 2), depending on the temperature. Furthermore, compound **3** can also be formed directly via path 2 in competition with the photochemically triggered process.

To gain deeper insight into the reaction scheme outlined above, we studied the independent thermal process corresponding to reaction path 2 in the absence of irradiation, both starting from the pyridine complex, **4**, (k_{-2}) and the acetonitrile complex, **3**, (k_2). The values obtained for k_{obs}

(15) Laurent, F.; Plantalech, E.; Donnadieu, B.; Jimenez, A.; Hernandez, F.; Martinez-Ripoll, M.; Biner, M.; Llobet, A. *Polyhedron* **1999**, *18*, 3321−3331.

(16) (a) Grant, G. J.; Salupobryant, T.; Holt, L. A.; Morrissey, D. Y.; Gray, M. J.; Zubkowski, J. D.; Valente, E. J.; Mehne, L. F. *J. Organomet. Chem.* **1999**, *587*, 207−214. (b) Cooper, S. R. *Acc. Chem. Res.* **1988**, *21*, 141−146.

(17) (a) Rodriguez, M.; Romero, I.; Llobet, A.; Deronzier, A.; Biner, M.; Parella, T.; Stoeckli-Evans, H. *Inorg. Chem.* **2001**, *40*, 4150−4156. (b) Wu, J. Z.; Ye, B. H.; Wang, L.; Ji, L. N.; Zhou, J. Y.; Li, R. H.; Zhou, Z. Y. *J. Chem. Soc., Dalton Trans.* **1997**, 1395−1401. (c) Coe, B. J.; Hayat, S.; Bedoes, R. L.; Helliwell, M.; Jeffrey, J. C.; Batten, S. R.; White, P. S. *J. Chem. Soc., Dalton Trans.* **1997**, 591−599. (d) Barqawi, K.; Llobet, A.; Meyer, T. J. *J. Am. Chem. Soc.* **1988**, *110*, 7751−7759.

(18) González, G.; Martinez, M.; Estevan, F.; García-Bernabé, A.; Lahuerta, P.; Peris, E.; Ubeda, M. A.; Díaz, M. R.; García-Granda, S.; Tejerina, B. *New. J. Chem.* **1996**, *20*, 83−94.

(19) Hecker, C. R.; Fanwick, P. E.; McMillin, D. R. *Inorg. Chem.* **1991**, *30*, 659−666.

Table 3. Kinetic Constants and Thermal Activation Parameters for the Studied Processes Indicated in Scheme 2

T/K	$10^4 \times (k_1K_{hv})_{app}/s^{-1}$	$10^5 \times k_2/s^{-1}$	$10^6 \times k_{-2}/s^{-1}$
294.6	0.59		
299.6	1.0 (1.1)[a]		
303.0	1.4		
303.8	1.8		
315.4		0.35	0.60[b]
323.5			2.2[c]
326.0		1.4	2.9[b]
333.0		3.6	7.5[b]
342.6		9.7	25[b]
348.0			52[c]
$\Delta H^{\#}$/kJ mol^{-1}		108 ± 3	121 ± 1
$\Delta S^{\#}$/J K^{-1} mol^{-1}		-8 ± 9	18 ± 3

[a] At higher-intensity continuous irradiation on a TIDAS instrument. [b] Obtained from the reaction of $[Ru(phen)(MeCN)([9]aneS_3)]^{2+}$ with pyridine in MeCN as the solvent. [c] Obtained from the reaction of $[Ru(phen)(py)([9]aneS_3)]^{2+}$ in MeCN.

are in agreement with the classical[20] equilibrium rate law: $k_{obs2} = k_2[\text{pyridine}] + k_{-2}$ (Supporting Information, Figure S2). The obtained first-order kinetic constants and their corresponding thermal activation parameters are collected in Table 3. From the Table, it can be observed that the ratio of k_2/k_{-2} is always higher than unity, thus manifesting the higher stability of the Ru−py complex with regard to that of the Ru−MeCN complex. The activation parameters that we obtained are in agreement with an interchange substitution mechanism that favors **4** with regard to **3** for enthalpic reasons: the breaking of a Ru(II)−N_{NCMe} bond and the formation of a Ru(II)−N_{py} bond is favored versus the inverse process. These activation parameters also agree with the I_d/I mechanism that has been previously described for ligand substitution reactions on Ru(II) centers.[21]

Under irradiation conditions and for temperatures below 304 K, the contribution of path 2 is practically negligible with regard to phototriggered[22] path 1 that takes place much faster. Table 3 presents the observed rate constants, k_{obs} ($(k_1K_{hv})_{app}$), in the range of 294.6−303.8 under these conditions, using **4** as the initial complex. Furthermore, this reaction was also carried out at different concentrations of pyridine and acetonitrile, leading to a constant value of the rate constant but with different absorption changes, as displayed in Table 4 at 303.8 K. From these results, it is clear that although the reaction rate constant is independent of both [py] and [MeCN] the associated absorbance changes decrease gradually on increasing the concentration of the leaving ligand. This suggests the existence of an equilibrium, prior to the substitution reaction (from intermediate to **3**), that is shifted toward **4** as [py] increases. This combination of facts implies that the MeCN molecule is already bonded to the Ru center in the photogenerated intermediate species.[23]

All of the data collected so far indicate that the intermediate generated in the phototriggered process, path 1 (Scheme 1), has two acetonitrile ligands coordinated to the ruthenium center. It is not probable that this species has both acetonitrile and pyridine ligands attached to the metal center because, according to the data obtained for path 2, such an intermediate would evolve toward the loss of MeCN and the formation of the original complex, $[Ru(phen)(py)([9]aneS_3)]^{2+}$. In this respect, the decreasing spectral changes obtained on increasing the amount of pyridine are also in accord with the existence of such a species.

Table 4. Values of k_{obs} with the Associated Absorbance Changes at Different Pyridine Concentrations in MeCN, [Ru] = 1.3×10^{-4} M, T = 303.8 K

[py]/M	[MeCN]/M	$10^4k_{obs}/s^{-1}$	$^{410\ nm}\Delta A$/au
0	19.0	1.67	0.31
0.21	18.7	1.69	0.29
0.42	18.4	1.63	0.29
0.83	17.7	1.71	0.23
1.04	17.4	1.72	0.20
2.08	15.8	1.66	0.15
3.12	14.2	1.71	0.07
6.20	9.40	1.72	0.01

Scheme 1

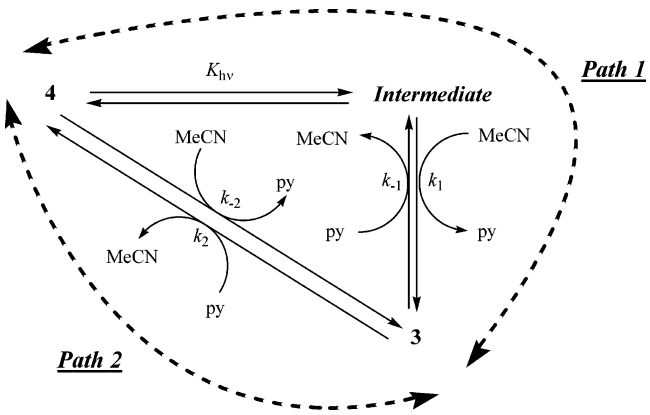

On the basis of all of the data described above and taking into consideration the literature related to dissociative substitution reactions for this type of complex,[7,9,24] the reaction mechanism presented in Scheme 2 is proposed.

The photochemical activation of the $[Ru(phen)(py)([9]aneS_3)]^{2+}$ complex (**4**) dissociatively evolves to an intermediate species where the monodentate ligand has been substituted by the solvent (MeCN). This dissociative process also involves the partial decoordination of one of the polydentate ligands, probably phen, and the sixth coordination position is occupied by the solvent (MeCN). A similar behavior has already been established for photochemically triggered reactions on Ru tris(diimine) complexes, where the products derived from the dissociation of a sterically hindered diimine are detected by NMR and HPLC.[25] The subsequent thermal chelation process produces then the final product, **3**. This type of dechelating behavior has also been established in other systems with formally labile ligands where no photo-

(20) González, G.; Martinez, M. *Inorg. Chim. Acta* **1995**, *230*, 67−75.
(21) (a) Rapaport, I.; Helm, L.; Merbach, A. E.; Bernhard, P.; Ludi, A. *Inorg. Chem.* **1988**, *27*, 873−879. (b) Leising, R. A.; Ohman, J. S.; Takeuchi, K. J. *Inorg. Chem.* **1988**, *27*, 3804−3809. (c) Arce Sagues, J. A.; Gillard, R. D.; Williams, P. A. *Transition Met. Chem. (Dordrecht, Neth.)* **1989**, *14*, 110.
(22) Rack, J. J.; Mockus, N. V. *Inorg. Chem.*, **2003**, *42*, 5792−5794.
(23) Bernhardt, P. V.; Gallego, C.; Martínez, M.; Parella, T. *Inorg. Chem.* **2002**, *41*, 1747−1754.
(24) Laemmel, A. C.; Collin, J. P.; Sauvage, J. P. *Eur. J. Inorg. Chem.* **1999**, 383−386.
(25) Tachiyashiki, S.; Ikesawa, H.; Mizumachi, K. *Inorg. Chem.* **1994**, *33*, 623−625.

Scheme 2

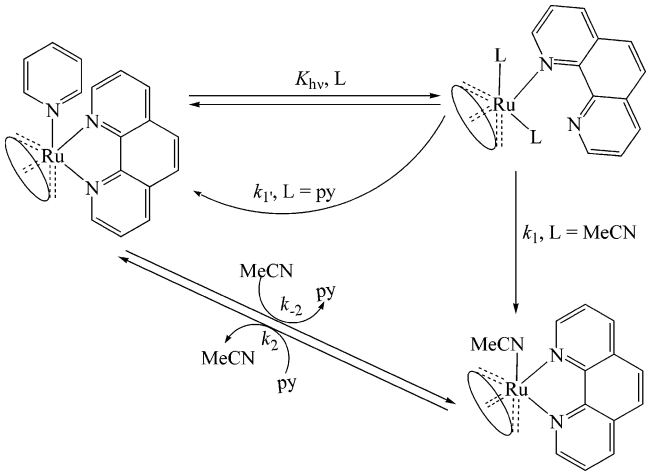

chemistry is involved.[26] We are at present carrying out further work to elucidate the relative importance of the chelating ligand and the solvent in the reaction mechanism.

It is important to mention here that for RuN_6-type complexes the substitution reaction kinetics are, as a general rule, much slower than the one just described. For instance, for the complex $[Ru(tpm)(py)_3]^{2+}$ (**7**) dissolved in MeCN under similar conditions as in **4**, no substitution at all is observed after a month of reaction time at room temperature. In the case of $[Ru(py)_3([9]aneS_3)]^{2+}$ (**6**) although the degree of congestion of the three facially coordinated py ligands is practically the same as in the case of $[Ru(tpm)(py)_3]^{2+}$, partial substitution of py by MeCN is observed. Therefore, steric effects can be discarded as the only cause of the observed enhanced lability. The electronic influence exerted by the very good π acceptor capabilities of the $[9]aneS_3$ ligand should be held responsible for the effects observed. At this point, it is tempting to attribute the differences to a simple trans effect of the macrocyclic ligand in a dissociatively activated substitution process. Nevertheless, the electronic effects of the py ligands cannot be discarded because for other types of complexes with $[9]aneS_3$ and highly σ-donating Cp ligands[16a] the trans effect operates, reinforcing the macrocyclic ligand bonding.

(26) (a) Basallote, M. G.; Durán, J.; Fernández-Trujillo, M. J.; González, G.; Máñez, M. A.; Martínez, M. *J. Chem. Soc., Dalton Trans.* **1999**, 3379−3383. (b) Basallote, M. G.; Durán, J.; Fernández-Trujillo, M. J.; González, G.; Máñez, M. A.; Martínez, M. *Inorg. Chem.* **1998**, *37*, 1623−1628.

Acknowledgment. This research has been financed by the MCYT of Spain through projects BQU2003-02884 and BQU2001-3205. A.L. is grateful to CIRIT Generalitat de Catalunya (Spain) for the Distinction award and the aid of SGR2001-UG-291. A.L. also thanks Johnson and Matthey for the $RuCl_3 \cdot xH_2O$ loan. X.S. is grateful for the award of a doctoral grant from the University of Girona.

Supporting Information Available: CIF files (**3**, CCDC no. 217745 and **4**, CCDC no. 217744) together with additional kinetic data. This material is available free of charge via the Internet at http://pubs.acs.org. The supplementary crystallographic data can also be obtained free of charge via www.ccdc.cam.ac.uk/conts/retrieving.html (or from the Cambridge Crystallographic Data Centre, 12, Union Road, Cambridge CB2 1EZ, U.K. Fax: +44 1223 336033. E-mail: deposit@ccdc.cam.ac.uk).

IC0497533